

Analytical Solutions for the Flexural Behavior of Metal Beams Strengthened with Prestressed Unbonded CFRP Plates

Kianmofrad, F.^{1*}, Ghafoori, E.², Motavalli, M.³ and Rahimian, M.⁴

¹ M.Sc., Arizona State University, School of Sustainable Engineering and the Built Environment, Arizona, USA.

² Assistant Professor, EMPA, Swiss Federal Laboratories for Materials Science and Technology, Structural Engineering Research Laboratory, Dübendorf, Switzerland.

³ Professor, EMPA, Swiss Federal Laboratories for Materials Science and Technology, Structural Engineering Research Laboratory, Dübendorf, Switzerland.

⁴ Professor, School of Civil Engineering, College of Engineering, University of Tehran, Tehran, Iran.

Received: 29 Jun. 2017;

Revised: 25 Dec. 2017;

Accepted: 25 Dec. 2017

ABSTRACT: Trapezoidal prestressed unbonded retrofit (TPUR) systems have been recently developed and tested. The authors have already developed a comprehensive and accurate analytical solution for the TPUR system that takes many system parameters into account. The main aim of this paper is to develop a simplified analytical solution for predicting the behavior of metal beams that have been strengthened with the TPUR system. The developed analysis method can be useful to engineers because of its simplicity. An energy approach based on Castigliano's theorems is used to study the flexural behavior of a steel beam retrofitted with the TPUR system. A parametric study was performed and the comparative results showed that the results using Castigliano's first theorem are in agreement with the results using the flexibility approach.

Keywords: Bridges, Energy Method, Flexibility Method, Metallic Beams, Prestressed CFRP Laminates, Strengthening.

INTRODUCTION

As infrastructure systems, especially bridges, become older and more prone to failure, the needs for effective retrofit methods are becoming more critical every day. There is currently a wide variety of retrofit methods being used for the extension of bridge service life, ranging from bonded carbon fiber reinforced polymer (CFRP) plates to unbonded steel tendons. Retrofitting methods can generally be classified into two

categories: prestressed and non-prestressed. One of the most significant advantages of using prestressed retrofit methods over non-prestressed methods is that in addition to the live load, prestressing transfers a portion of the dead load into the retrofitting system, and thus the load capacity of the structure experiences greater improvement than if a non-prestressed retrofit system is used (Ghafoori and Motavalli, 2013).

Another way to classify retrofitting systems is by their attachment to the

* Corresponding author E-mail: Farrokh.Kianmofrad@asu.edu

structure, which can be based on bonded or unbonded methods. Bonded methods use adhesives to attach the retrofit components to the original structure. However, bonded methods require a clean, smooth, and polished surface to function properly. On the other hand, unbonded methods, such as the prestressed unbonded retrofit (PUR) systems discussed in this paper, are much more adaptable and can be used on a wider variety of structures in various applications (e.g., bridges, heritage buildings, etc.), and in different difficult conditions (e.g., corroded, cracked, or uneven surfaces, etc.). On a member with smooth or bumpy surface (such as an oxidized steel beam), the contact PUR (CPUR) system or the flat PUR (FPUR) system can be used, while on a member with an obstructed surface (such as bolted members), the trapezoidal PUR (TPUR) system or the triangular PUR (TriPUR) system can be utilized. Importantly, the type of PUR system does not result in any significant change of behavior; what is important in the system is the prestress level in the CFRP plate(s) (Kianmofrad et al., 2017). Therefore, the tensions in the system, and the resulting strains and deflections, must be calculated using an accurate approach.

In the past, the research and application efforts of scholars and engineers using FRP-based prestressed retrofitting systems were focused on concrete structures, and less attention was paid to applying these prestressing techniques to metal structures (U.S. Department of Transportation, 1986). In the recent decades, however, although the research on the fiber reinforced concrete (FRC) and external strengthening methods using FRP is still going on (Rashid Dadash and Ramezaniapour, 2014; Saleh Jalali and Shadafza, 2016; Soranakom and Mobasher, 2007), more investigations have been conducted on metal members strengthened by prestressed retrofitting systems such as those using FRP materials (Park et al., 2010;

Ponnada and Vipparthy, 2013; Schnerch and Rizkalla, 2008).

In general, the strengthening of metal structures is performed to mitigate static or fatigue problems. Static problems include insufficient yield or ultimate capacity of the member (e.g., due to increased traffic loads or reduced member cross-section resulting from corrosion), buckling (e.g., lack of sufficient lateral constraints), and the like. To this end, a series of studies have been performed to determine the effect of CFRP strengthening on the yield and ultimate capacity (Ghafoori, 2013; Ghafoori and Motavalli, 2013; Ghafoori and Motavalli, 2015a; Kianmofrad et al., 2017), and buckling strength (Ghafoori and Motavalli, 2015b,c) of steel members.

The progress of fatigue damage in steel bridge members can be divided into two different phases: crack initiation and crack propagation. Recent studies by Ghafoori, 2015; Ghafoori and Motavalli, 2016; Ghafoori et al., 2015a; Ghafoori et al., 2015c; Ghafoori et al., 2014) have shown that CFRP material can be successfully employed to prevent fatigue crack initiation in old steel members. Based on the results of these studies, Ghafoori et al. (2015a) developed a CFRP retrofit system and a proactive fatigue design approach to prevent the initiation of fatigue cracks in the riveted girders of a 120-year-old railway bridge in Switzerland. Furthermore, there exists a large body of research on methods for arresting existing fatigue cracks in steel members using prestressed CFRP materials (Aljabar et al., 2016, 2017; Fernando et al., 2010; Ghafoori and Motavalli, 2011; Ghafoori et al., 2012; Hosseini et al., 2016).

Ghafoori et al. (2012) investigated the effect of prestressed CFRP strengthening plates on the fatigue life of a notched steel beam, concluding that the use of CFRP prestressing could significantly increase the fatigue life of the beam and improve the performance of the member in terms of both

strength and ductility. Similar studies show the same results and have reported an increase in fatigue life of strengthened damaged members between 10 to 20 times that of the unstrengthening members, and in some cases even complete crack arrest (Ghafoori et al., 2012; Ghafoori et al., 2012; Huawen et al., 2010; Täljsten et al., 2009; Tavakkolizadeh and Saadatmanesh, 2003). The advantages of CFRP materials for strengthening purposes (such as a high strength-to-weight ratio, excellent corrosion and fatigue resistance, etc.) together with the recent accessibility of high modulus CFRP strips at reduced prices has made it increasingly feasible to strengthen steel structures (Schnerch and Rizkalla, 2008).

Given the recent widespread use of prestressed retrofitting systems, many researchers have examined these systems using analytical approaches for predicting the behavior of elements retrofitted using CFRP materials. So far, a number of researchers have suggested analytical solutions for the behavior of prestressed bonded reinforced (PBR) systems for metal beams (Al-Emrani and Kliger, 2006; Benachour et al., 2008; Ghafoori and Motavalli, 2013; Kerboua and Benmoussat, 2011). In these studies, different aspects of metal members retrofitted by PBR systems, such as the effect of shear deformation, the stress induced in the cohesive layer, and the effect of cracks in the strengthened member have been examined.

Recently, a prestressed unbonded retrofit (PUR) system for CFRP strengthening of metallic girders has been developed by Ghafoori and Motavalli (2015d). The authors proposed an analytical solution based on the assumption that the deformation in the steel beam is negligible compared to that in the CFRP plates (i.e., the rigid-beam assumption). From this assumption, they derived formulations to calculate the desired CFRP prestress level. Though this calculation method was easy to use, it was not very

accurate for more sensitive applications that require a precise result. Kianmofrad et al. (2017) presented a comprehensive and accurate solution for this type of retrofitting system, taking into account many parameters (i.e., the beam deformation due to prestressing, the loading distance, the geometric and material properties of the PUR system and the beam itself, and so forth). They showed that the specific type of PUR system used has a negligible effect on the increased strength of the member, and that the greatest influence on the system performance is the pre-stress level applied (Kianmofrad et al., 2017). Although their method is very accurate and can be applied to many different types of PUR systems, it is complex and requires the use of many parameters. The present study aims to develop a simple and relatively accurate analytical solution for predicting the behavior of metal beams strengthened with a PUR system. It is expected that this solution will be useful for engineers due to its simplicity.

OBJECTIVES AND ASSUMPTIONS

The main objective of this paper is to evaluate two analytical solutions using energy approaches based on Castigliano's first and second theorems. The results of these analytical solutions are then compared with other analytical and experimental results found in the literature. Kianmofrad et al. (2017) presented several types of PUR systems, among them the trapezoidal PUR (TPUR) system has been chosen to be addressed in this research, on the basis of the extensive experimental, numerical, and analytical research in existence using this type of system. The TPUR system setup and its different parameters are depicted in figure 1 (Kianmofrad et al., 2017). More detailed discussions of this system can be found in (Ghafoori and Motavalli, 2015a; Kianmofrad et al., 2017). To summarize, in the TPUR

system, the ends of the CFRP plates are fastened inside a pair of friction clamps that transfer the tensile force from the CFRP plates to the beam in the form of bending moment, shear, and axial forces. By increasing the deviator height, e , the prestress level in the beam is increased and an upward deflection is applied to the beam (i.e., “bow-like” deformation). The deviator height is increased until the desired prestress level in the CFRP plates is achieved. During the prestressing procedure, there should be no external live load on the beam. As mentioned earlier, Kianmofrad et al. (2017) have already presented an analytical solution for the TPUR system based on the flexibility approach. As the TPUR system has one degree of indeterminacy, to solve the system, they assumed that the CFRP plates are cut from the beam to make the system statically determinate, and then the beam and CFRP plates are analyzed separately, using a

compatibility equation, to obtain the forces and stresses. In this paper, the same assumptions are made to solve the system using other analytical approaches. These assumptions are mentioned here briefly.

A glance to Figure 1 reveals that the system is symmetric about the mid span of the beam, so it is sufficient to perform these calculations for only half of the system. Furthermore, it is assumed that the CFRP plates exhibit only axial deformation and that their bending stiffness is negligible, and the friction between the CFRP plate and the deviator is neglected (Kianmofrad et al., 2017; Park et al., 2010). Although it is considered that all materials behave in a linear-elastic manner and possess homogenous distribution, there remains a geometrically non-linear behavior due to the large geometric deformation in the CFRP plates, caused by the changes in the length of the deviators (see Figures 1 and 2).

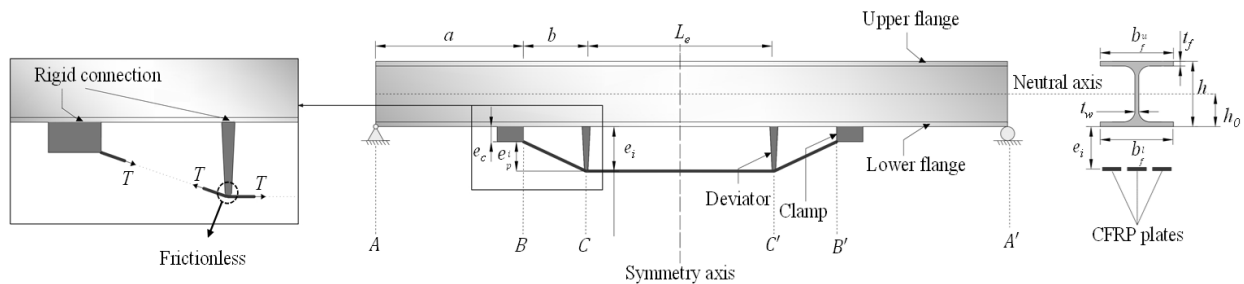


Fig. 1. The parameters used in the TPUR system (Kianmofrad et al., 2017)

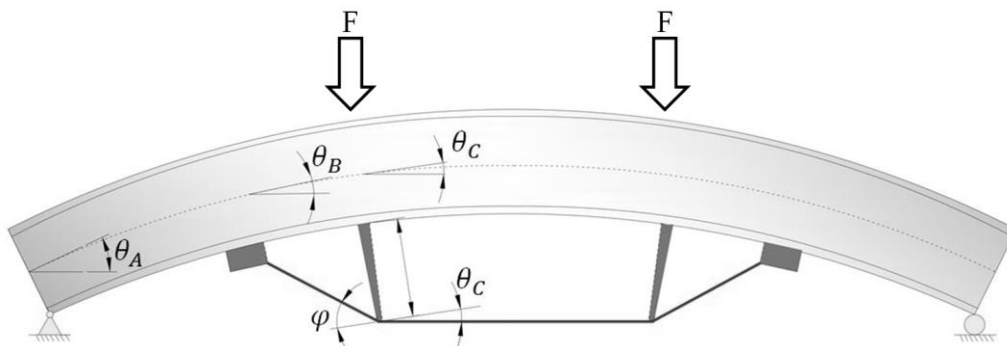


Fig. 2. Beam deformation after prestressing and at the beginning of loading. As the external loading, F , increases, the upward deflection will change to downward deflection (Kianmofrad et al., 2017)

ENERGY APPROACH USING CASTIGLIANO'S FIRST THEOREM

There are several methods for solving an engineering problem based on the energy approach, such as Castigliano's theorems and virtual work. Castigliano's second theorem is likely to yield inaccurate results in this situation because of the geometrically non-linear behavior of the system (Timoshenko and Young, 1965). Similarly, other energy methods (such as the virtual-work or the least-work methods) are not applicable here (Boresi et al., 1993). Therefore, Castigliano's first theorem is used to evaluate the strengthened system.

According to Castigliano's first theorem, in an elastic structure, whether linear or non-linear, the partial derivative of the strain energy with respect to any displacement in the structure is equal to the load(s) applied in the direction of displacement, shown by Eq. (1).

$$\frac{\partial U}{\partial \Delta_i} = P_i \quad (1)$$

where U is the strain energy, and Δ_i and P_i are the displacement (or rotation) and the force (or moment), respectively, at node i .

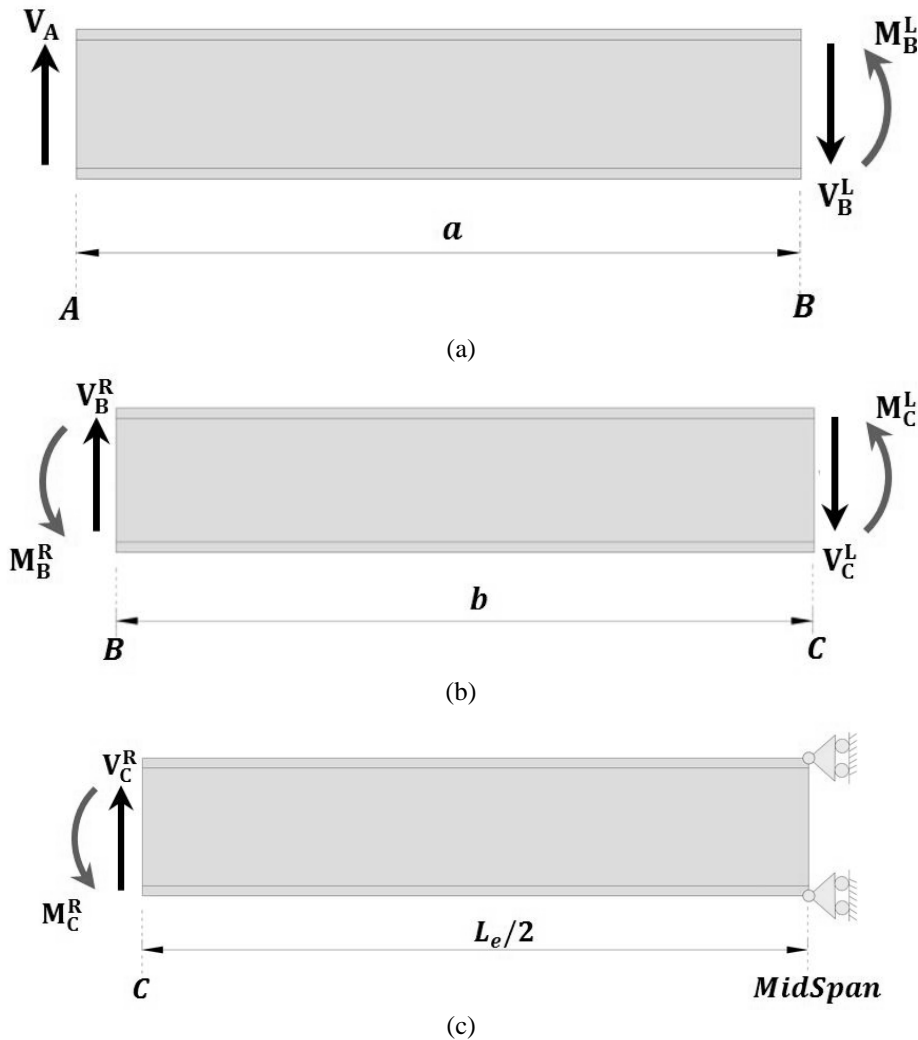


Fig. 3. For analysis, the beam is separated into several segments (a,b,c) and the energy of each segment is calculated (superscripts R and L refer to the right side and the left side, respectively, of the i^{th} part)

To apply this method, the beam is divided into several segments, as shown in Figure 3. After calculating the strain energy for each segment, the total strain energy of the system can be achieved by summing up the strain energy of all segments. In general, the beam under consideration can be divided into five segments, but due to symmetry, segments $A'B'$ and $B'C'$ are similar to segments AB and BC ; accordingly, the energy calculation is done for only half of the beam and the result is doubled. In general, the strain energy for a beam element (i.e., a one dimensional element) can be obtained using slope-deflection equations (Hibbeler, 2014; Rahimian and Ghorbani Tanha, 2002) as follows (Figure 4)

$$U_{ij} = \frac{1}{2}M_i\theta_i + \frac{1}{2}M_j\theta_j + \frac{1}{2}R_j\delta_{ji} \quad (2)$$

$$U_{ij} = 2E_s k_{ij}(\theta_i^2 + \theta_i\theta_j + \theta_j^2) - 6E_s k_{ij}\psi_{ij}(\theta_i + \theta_j) + 6E_s k_{ij}\psi_{ij}^2 \quad (3)$$

in Eq. (2) U_{ij} : is the strain energy in beam segment ij (i.e., between nodes i and j), M_i and θ_i : are moment and rotation at node i , respectively, and are defined as positive in the counter-clockwise direction. R_j : is the support reaction at node j , and δ_{ji} : is the relative vertical displacement between nodes i and j , which can be calculated as follows:

$$\delta_{ij} = \delta_j - \delta_i \quad (4)$$

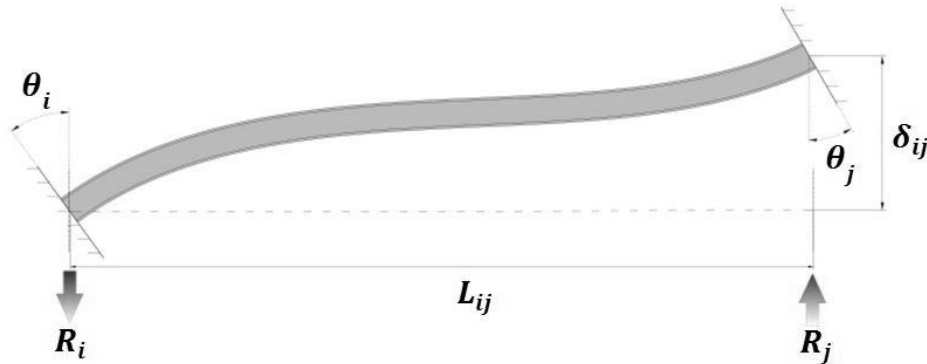


Fig. 4. The parameters used in Eqs. (2-3), based on the slope-deflection method

in Eq. (3), E_s : is the Young's modulus of steel, and ψ_{ij} : is the rotation of beam segment ij where:

$$\psi_{ij} = \frac{\delta_{ij}}{L_{ij}} \quad (5)$$

and k_{ij} : is the span-stiffness of the beam segment ij , which represents the beam resistance against bending and is used for abbreviation. It is noted that, this is not a real stiffness, based on the stiffness definition, and its dimension is different from stiffness definition.

$$k_{ij} = I/L_{ij} \quad (6)$$

where I : is the moment of inertia of the beam cross-section, and L_{ij} : is the length of beam segment ij .

Accordingly, for each beam segment, as shown in Figure 3, Eq. (3) can be rewritten as

$$U_{AB} = U_{A'B'} = 2E_s k_{AB}(\theta_A^2 + \theta_A\theta_B + \theta_B^2) - 6E_s k_{AB}\psi_{AB}(\theta_A + \theta_B) + 6E_s k_{AB}\psi_{AB}^2 \quad (7)$$

$$U_{BC} = U_{B'C'} = 2E_s k_{BC}(\theta_B^2 + \theta_B\theta_C + \theta_C^2) - 6E_s k_{BC}\psi_{BC}(\theta_B + \theta_C) + 6E_s k_{BC}\psi_{BC}^2 \quad (8)$$

$$U_{CC'} = 2E_s k_{CC'}(\theta_C^2 - \theta_C^2 + \theta_C^2) = 2E_s k_{CC'}\theta_C^2 \quad (9)$$

The beam clearly has ten degrees of freedom (DOF), but given the symmetry, the number of DOFs can be decreased by five (i.e., $\theta_A, \theta_B, \theta_C, \delta_B$, and δ_C). The CFRP plate has only one longitudinal DOF (i.e., Δ), therefore its strain energy can be obtained as follows:

$$U_P = \frac{1}{2} \frac{E_P A_P}{L_i} \Delta^2 \quad (10)$$

where E_P and A_P : represent Young's modulus and the total cross-sectional area of the CFRP plate(s), respectively, in which the subscript p indicates the CFRP plate, and L_i : is the initial length of the CFRP plate before pre-stressing, which can be written as

$$L_i = L_e + 2\sqrt{b^2 + (e_i - e_c)^2} \quad (11)$$

where e_c : is the clamp thickness, e_i : is the initial length of the deviators, b : is the length of the beam segment BC , and L_e : is the length of the beam segment CC' (these parameters are depicted in Figure 1).

The total strain energy of the system can be calculated by summing the strain energy for each segment, i.e., Eqs. (7-10), as follows:

$$\begin{aligned} U &= U_{AB} + U_{BC} + U_{CC'} + U_{B'C'} \\ &\quad + U_{A'B'} + U_f \\ &= 2U_{AB} + 2U_{BC} + U_{CC'} \\ &\quad + U_P \\ &= 2(2E_s k_{AB} (\theta_A^2 \\ &\quad + \theta_A \theta_B + \theta_B^2) \\ &\quad - 6E_s k_{AB} \psi_{AB} (\theta_A + \theta_B) \\ &\quad + 6E_s k_{AB} \psi_{AB}^2) \\ &\quad + 2(2E_s k_{BC} (\theta_B^2 \\ &\quad + \theta_B \theta_C + \theta_C^2) \\ &\quad - 6E_s k_{BC} \psi_{BC} (\theta_B + \theta_C) \\ &\quad + 6E_s k_{BC} \psi_{BC}^2) \\ &\quad + 2E_s k_{CC'} \theta_C^2 \\ &\quad + \frac{1}{2} \frac{E_P A_P}{L_i} \Delta^2 \end{aligned} \quad (12)$$

For the rotational DOFs, according to Castigliano's first theorem:

$$\frac{\partial U}{\partial \theta_A} = 0 \quad (13)$$

$$\frac{\partial U}{\partial \theta_B} = 2M_B \quad (14)$$

$$\frac{\partial U}{\partial \theta_C} = 2M_C \quad (15)$$

and for the displacement DOFs,

$$\frac{\partial U}{\partial \delta_B} = -2V_B \quad (16)$$

$$\frac{\partial U}{\partial \delta_C} = -2V_C \quad (17)$$

$$\frac{\partial U}{\partial \Delta} = T \quad (18)$$

where M_C : is the moment at section C (and C'), M_B : is the moment at section B (and B'), V_C : is the shear force at section C (and C'), V_B is the shear force at section B (and B') and T is the tensile force in the CFRP plate. The moment at sections B and C (also B' and C') can be calculated as follows:

$$M_B = T(d + h_0) \cos \varphi \quad (19)$$

and

$$M_C = T(e + h_0)(\cos \theta_C - \cos \varphi) \quad (20)$$

where h_0 : is the distance from the neutral axis to the bottom of the beam lower flange. Parameter d is shown in Figure 5 and can be obtained as

$$d = e_c - (\delta_{BC}^F - \delta_{BC}^T) \quad (21)$$

where

$$\delta_{BC}^F = \frac{F \cdot b^3}{3E_s I} + \frac{(F \cdot a) \cdot b^2}{2E_s I} \quad (22)$$

and

$$\delta_{BC}^T = \frac{T \sin \varphi \cdot b^3}{3E_s I} + \frac{T \cos \varphi (d + h_0)b^2}{2E_s I} \quad (23)$$

where δ_{BC}^F and δ_{BC}^T : are the relative vertical displacement of section B toward section C caused by the external loading, F, and the tensile force in the CFRP plate, T, respectively. Also, as

$$\sin \varphi = \frac{e - d}{\sqrt{b^2 + (e - d)^2}} \quad (24)$$

and

$$\cos \varphi = \frac{b}{\sqrt{b^2 + (e - d)^2}} \quad (25)$$

the shear forces at sections B and C (as well as B' and C') can be obtained as follows:

$$V_B = T \sin \varphi \quad (26)$$

and

$$V_C = (F - T \sin \varphi) \quad (27)$$

Given that there are seven unknown parameters (i.e., $\theta_A, \theta_B, \theta_C, \delta_B, \delta_C, \Delta$, and d), there needs to be seven equations in order to solve the system of equations. However, there are only six equations (Eqs. (13-18)). Therefore, a compatibility equation is introduced as follows:

$$\Delta = L - L_i = 2 \left(\sqrt{(e - d)^2 + b^2} - \sqrt{(e_i - e_c)^2 + b^2} - (e + h_0) \sin \theta_c \right) \quad (28)$$

The above equation is a geometrical relationship representing the length change in the CFRP plate after pre-stressing and resulting system deformation.

Substituting Eqs. (12) and (19-28) into Eqs. (13-18), and after some calculation, a system of seven equations with seven

unknown parameters is achieved as follows:

$$2[2E_s k_{AB}(2\theta_A + \theta_B) - 6E_s k_{AB} \psi_{AB}] = 0 \quad (29)$$

$$2[2E_s k_{AB}(2\theta_B + \theta_A) - 6E_s k_{AB} \psi_{AB}] + 2[2E_s k_{BC}(2\theta_B + \theta_C) - 6E_s k_{BC} \psi_{BC}] = 2T \cos \varphi (d + h_0) \quad (30)$$

$$2[2E_s k_{BC}(2\theta_C + \theta_B) - 6E_s k_{BC} \psi_{BC}] + 4E_s k_{CC'} \theta_C = 2T (\cos \theta_C - \cos \varphi) (e + h_0) \quad (31)$$

$$2 \left[-\frac{6E_s k_{AB}}{L_{AB}} (\theta_A + \theta_B) + \frac{12E_s k_{AB} \psi_{AB}}{L_{AB}} \right] + 2 \left[\frac{6E_s k_{BC}}{L_{BC}} (\theta_B + \theta_C) - \frac{12E_s k_{BC} \psi_{BC}}{L_{BC}} \right] = -2T \sin \varphi \quad (32)$$

$$2 \left[-\frac{6E_s k_{BC}}{L_{BC}} (\theta_B + \theta_C) + \frac{12E_s k_{BC} \psi_{BC}}{L_{BC}} \right] = -2(F - T \sin \varphi) \quad (33)$$

$$\frac{2E_f A_f}{L_i} \left[\sqrt{(e - d)^2 + b^2} - \sqrt{(e_i - e_c)^2 + b^2} - (e + h_0) \sin \theta_c \right] = T \quad (34)$$

$$d = e_c - \left(\frac{F \cdot b^3}{3E_s I} + \frac{(F \cdot a) \cdot b^2}{2E_s I} - \frac{T \sin \varphi \cdot b^3}{3E_s I} - \frac{T \cos \varphi (d + h_0)b^2}{2E_s I} \right) \quad (35)$$

By substituting the parameters F and e into above system of equations, the other unknown parameters can be calculated. To simulate the behavior of the TPUR system during pre-stressing prior to the application of external loading, F should be set to zero (i.e., $F = 0$) in above equations. Therefore, it can be seen that by increasing the deviator height, e , the tensile force in the system increases as well. Considering the fact that the middle segment of the beam, CC' , is like a simply supported beam upon which two bending moments (M_C and $M_{C'}$) are applied at its ends, the midspan deflection, δ_M , can be

calculated as

$$\delta_M = - \left(\frac{M_c L_e^2}{8E_s I} + \delta_c \right) \quad (36)$$

ENERGY APPROACH USING CASTIGLIANO'S SECOND THEOREM

In the previous section, a solution for determining the behavior of the TPUR system based on Castigliano's first theorem was introduced. However, due to the number of DOFs and the associated necessity of forming a system of algebraic equations, this approach can be complicated, and thus is not preferable for practical purposes, especially when applied to systems in which the number of DOFs is greater than the degree of indeterminacy. For these reasons, the use of Castigliano's second theorem is more popular among engineers, although it does not give very accurate solutions for non-linear systems. The aim of this, is to provide a basis for comparison between different methods. Although, it is correct that the second theorem is not appropriate for non-linear behaviors, but still in some applied engineering situations, that the highest accuracy is not necessary, such as initial estimations for the sections or deflections, we are able to use some estimations and assumptions to simplify the complicated problems for the engineers. For purposes of comparison to the more complex method, in

this section, an approximate solution based on Castigliano's second theorem is presented.

Given the fact that the materials used in this study are considered to be linear-elastic materials, the strain energy can be written as (Boresi et al., 1993),

$$U = \int_V U_0 dV \quad (37)$$

$$U^* = \int_V U_0^* dV \quad (38)$$

For linear-elastic materials,

$$\sigma_{ij} = E \varepsilon_{ij} \quad (39)$$

Therefore

$$U_0 = \int_0^{\varepsilon_{ij}} \sigma_{ij} d\varepsilon_{ij} = \int_0^{\varepsilon_{ij}} E \varepsilon_{ij} d\varepsilon_{ij} \quad (40)$$

$$= \frac{1}{2} \varepsilon_{ij}^2 = \frac{1}{2} \sigma_{ij} \varepsilon_{ij}$$

and

$$U_0^* = \int_0^{\sigma_{ij}} \varepsilon_{ij} d\sigma_{ij} = \int_0^{\sigma_{ij}} \frac{\sigma_{ij}}{E} d\sigma_{ij} \quad (41)$$

$$= \frac{1}{2E} \sigma_{ij}^2 = \frac{1}{2} \sigma_{ij} \varepsilon_{ij}$$

Therefore $U_0 = U_0^*$, ε and σ : are strain and stress, respectively, and U^* : is the complementary strain energy, shown in Figure 6.

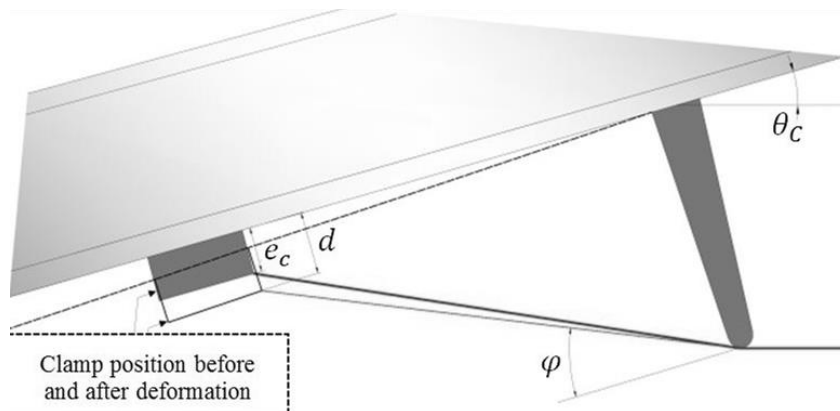


Fig. 5. Relative displacements at sections B (clamp position) and C (deviator position)

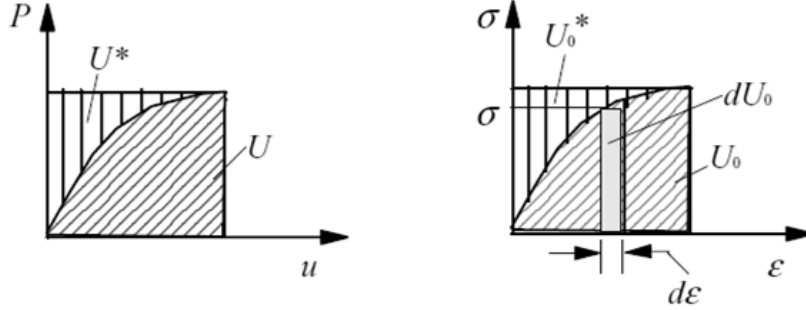


Fig. 6. Schematic illustrations of the energy method concept for the development of force-displacement and stress-strain curves (Boresi et al., 1993)

In a beam with cross-section A,

$$N(x) = \int_A \sigma_{xx} dA \quad (42)$$

$$M(x) = \int_A \sigma_{xx} Z dA \quad (43)$$

and

$$V(x) = \int_A \sigma_{xz} dA \quad (44)$$

The strain energy caused by the bending moment is calculated as follows:

$$U_{0M}^* = \int_0^{\sigma_{xx}} \epsilon_{xx} d\sigma_{xx} \quad (45)$$

$$\begin{aligned} U_M^* &= \int_V \frac{1}{2E} \sigma_{xx}^2 dV \\ &= \frac{1}{2E} \int_0^L \frac{M^2}{I^2} \left[\int_A y^2 dA \right] dx \\ &= \frac{1}{2EI} \int_0^L M^2(x) dx \end{aligned} \quad (46)$$

in the same manner,

$$U_V^* = \frac{1}{2GA_s} \int_0^L V^2(x) dx \quad (47)$$

and

$$U_N^* = \frac{1}{2EA_s} \int_0^L N^2(x) dx \quad (48)$$

where U_M^* , U_N^* , and U_V^* are the strain energy due to bending, axial, and shear deformations, respectively, and A_s is the effective shear cross-section area. It is clear that in this case there is no twisting deformation, and the amount of axial deformation is negligible compared to the bending and shear deformations. Therefore, the total strain energy U^* , can be obtained as follows:

$$U^* = U_M^* + U_V^* \quad (49)$$

Note that there is only longitudinal deformation in the CFRP plate. Therefore, the strain energy in the CFRP plate, U_P^* , can be written as

$$U_P^* = U_{NP}^* \quad (50)$$

in this method, as in the previous method, the beam is divided into several segments.

Strain Energy in Beam Segment BC and $B'C'$

The beam segment AB (and $A'B'$) does not exhibit any deformation during pre-stressing as there are no external forces or bending moments applied to this segment, and accordingly its strain energy is equal to zero. However, there are bending and shear deformations in beam segment BC (and $B'C'$). The strain energy for bending deformation is:

$$U_{M(BC)}^* = \frac{1}{2EI} \int_0^b M_{(BC)}^2(x) dx \quad (51)$$

According to the external loading applied to this segment (as depicted in Figure 7),

$$M_B = T \cos \varphi (e_c + h_0) \quad (52)$$

and

$$M_{BC}(x) = M_B + xT \sin \varphi \quad (53)$$

Substituting Eq. (53) into Eq. (51),

$$U_{M(BC)}^* = \frac{T^2}{2EI} \left[b \cos^2 \varphi (e_c + h_0)^2 + \frac{b^3 \sin^2 \varphi}{3} + b^2 \sin \varphi \cos \varphi (e_c + h_0) \right] \quad (54)$$

Strain energy for shear deformation can be obtained as

$$U_{V(BC)}^* = \frac{f_s}{2GA} \int_0^b V^2(x) dx \quad (55)$$

Because the shear force remains unchanged along this segment,

$$V(x) = V = T \sin \varphi \quad (56)$$

$$U_{V(BC)}^* = \frac{bT^2 \sin^2 \varphi}{2GA_s} \quad (57)$$

The total energy in this segment can be expressed as

$$U_{(BC)}^* = U_{V(BC)}^* + U_{M(BC)}^* \quad (58)$$

Strain Energy in Beam Segment CC'

Given the symmetric loading, there is no shear deformation in this segment. Therefore, the only strain energy is due to bending deformation,

$$U_{(cc')}^* = U_{M(cc')}^* = \frac{1}{2EI} \int_0^{L_e} M_{(cc')}^2(x) dx = \frac{M_c^2 L_e}{2EI} \quad (59)$$

where L_e is the length of the beam segment CC' , and M_c can be calculated as follows

$$M_c = M_B + T \sin \varphi \times b + T(\cos \theta_c - \cos \varphi)(e + h_0) = T[\cos \varphi (e_c + h_0) + b \sin \varphi + (e + h_0)(\cos \theta_c - \cos \varphi)] \quad (60)$$

and θ_c is also a function of M_c ,

$$\theta_c = \frac{M_c L_e}{2EI} \quad (61)$$

Strain Energy in the Cfrp Plate and the Total Strain Energy

Because there is only longitudinal deformation in the CFRP plate,

$$U_{(p)}^* = U_{N(p)}^* = \frac{1}{2E_p A_p} \int_0^{L_i} N^2(x) dx = \frac{T^2 L_i}{2E_p A_p} \quad (62)$$

where L_i is the initial length of the plate.

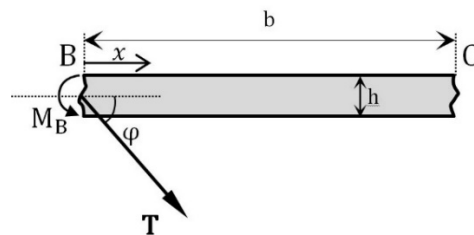


Fig. 7. External loading on beam segment BC

The total strain energy of the system can now be obtained as follows:

$$U^* = 2U_{(BC)}^* + U_{(CC')}^* + U_{(P)}^* \quad (63)$$

Finally, after doing some calculations,

$$\begin{aligned} \frac{\partial U^*}{\partial T} = \frac{2T}{EI} & \left[b \cos^2 \varphi (e_c + h_0)^2 \right. \\ & + \frac{b^3 \sin^2 \varphi}{3} \\ & + b^2 \sin \varphi \cos \varphi (e_c \\ & + h_0) \left. \right] + \frac{2Tb \sin^2 \varphi}{GA_s} \\ & + \frac{TL_i}{E_p A_p} \\ & + \frac{TL_e}{EI} [\cos \varphi (e_c + h_0) \\ & + b \sin \varphi + (e \\ & + h_0)(\cos \theta_c \\ & - \cos \varphi)]^2 \end{aligned} \quad (64)$$

and

$$\frac{\partial U^*}{\partial T} = \Delta \quad (65)$$

where

$$\begin{aligned} \Delta = & \sqrt{b^2 + (e - e_c)^2} \\ & - \sqrt{b^2 + (e_i - e_c)^2} \\ & - (e + h_0) \sin \theta_c \end{aligned} \quad (66)$$

in which Δ : is the change in length of the CFRP plate. After substituting Eqs. (65-66) into Eq. (64), T can be obtained in terms of the deviator length, e .

COMPARISON OF RESULTS FROM CASTIGLIANO'S FIRST AND SECOND THEOREMS

The prestress results for an example retrofitted steel I-beam strengthened by a TPUR system are obtained using Matlab programs based on Castigliano's first and second theorems and are then compared. The

dimensions and material properties used in the mathematical simulations are similar to those given in (Kianmofrad et al., 2017) and are listed in Tables 1 and 2.

Figure 8 shows the tensile stress in the CFRP plate as a function of deviator height, e . From this figure, it can be seen that as the deviator height increases, the tensile force in the CFRP plate increases as well. However, as mentioned previously, in the absence of external loading, the relationship between T and e is nonlinear. Ghafouri and Motavalli (2015a) have developed a method for calculating the tensile force and prestress level as a function of the eccentricity, e , based on the assumption that the beam is rigid, and therefore has negligible upward deflection when subjected to a negative bending moment. Figure 8 shows the results from their research, based on the rigid beam assumption, as well as the results from Kianmofrad et al. (2017), obtained using the flexibility method, compared with the results from the current research calculated using the energy method based on Castigliano's theorems.

From Figures 9-10, it can be observed that there is no difference between results obtained using the flexibility method and Castigliano's first theorem. It should be noted that although both of these methods are giving the same answers but the approaches are quite different. Kianmofrad et al. have used an analytical approach based on the Flexibility (Force) method while in the current research energy approaches have been investigated. As was expected, the results obtained using Castigliano's second theorem are not very accurate, predicting a tension in the CFRP plate around 12% lower than the value calculated using either Castigliano's first theorem or the flexibility method. Similarly, the results obtained using the rigid beam assumption are fairly imprecise as well, predicting the tension in the CFRP plate about 13% higher than determined using the more exact methods.

Table 1. Beam dimensions and geometric parameters of the simulated TPUR system (in mm) (see Figure 1)

| System | Section | L_b^* | a | b | Le | l | h | b_f^u | b_f^l | t_w | t_f | e_c | e_p^i | $e_i = e_p^i + e_c$ |
|--------|---------|---------|-----|-----|------|-----|-----|---------|---------|-------|-------|-------|---------|---------------------|
| TPUR | IPB1240 | 5000 | 825 | 825 | 1700 | 0 | 230 | 240 | 230 | 7.5 | 12 | 55 | 104 | 159 |

Table 2. Mechanical properties of the CFRP and steel, and the steel section properties

| System | σ_p^U (MPa) | E_p (GPa) | E_s (GPa) | A_p (mm ²) | A_s (mm ²) | I_s (mm ⁴) |
|--------|--------------------|-------------|-------------|--------------------------|--------------------------|--------------------------|
| TPUR | 2450 | 158.5 | 209 | 180 | 7350 | 7340e4 |

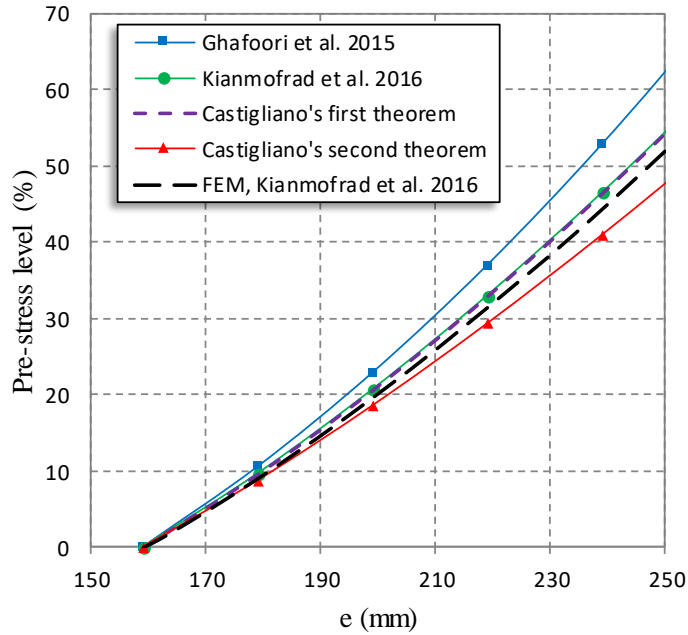


Fig. 8. Prestress level in the CFRP plate in terms of the deviator height e , calculated using different methods

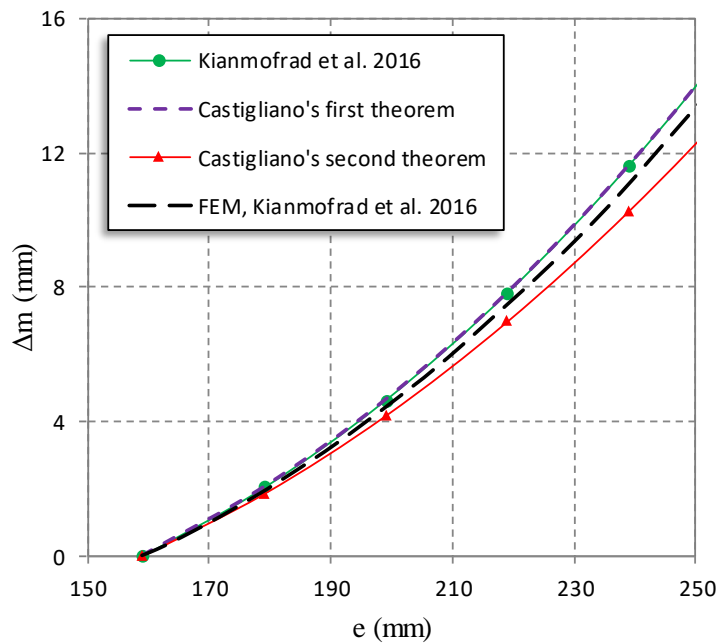


Fig. 9. Mid span deflection in terms of the deviator height e , calculated using different methods

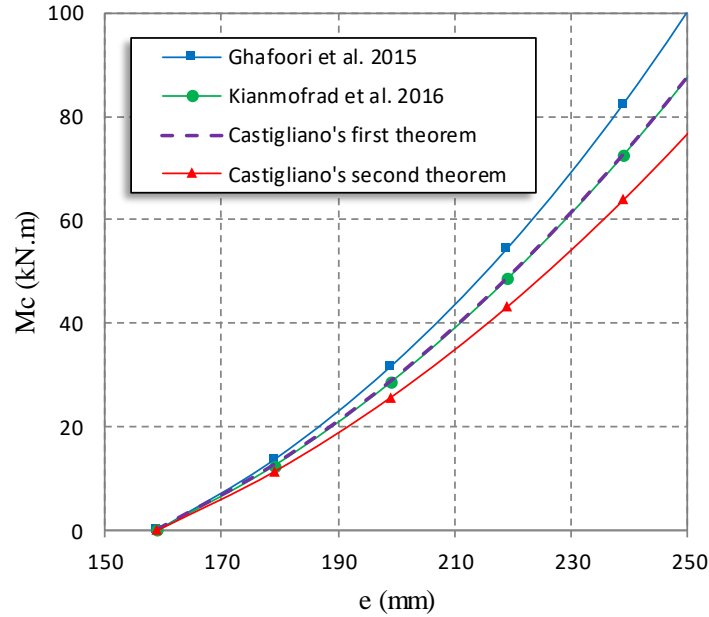


Fig. 10. Bending moment at mid span in terms of deviator height (e), obtained using different methods

Figure 9 illustrates the mid span deflection, δ_M , as a function of deviator height, e . From this figure, it can be seen that the mid span deflection anticipated using Castigliano's second theorem is smaller than that obtained using either Castigliano's first theorem or the flexibility method. The use of Castigliano's second theorem predicts the system behavior to be around 12.5% stiffer than determined using the flexibility method.

Because the tensile force in the CFRP plate obtained using Castigliano's second theorem is smaller than when determined using more exact methods, it would not be unexpected that the bending moment at mid span would be smaller as well. Figure 10 illustrates the bending moment at beam mid span in terms of the deviator height. Surprisingly, according to this figure, the predicted bending moment when using the rigid beam assumption is about 16% higher than when using more exact methods.

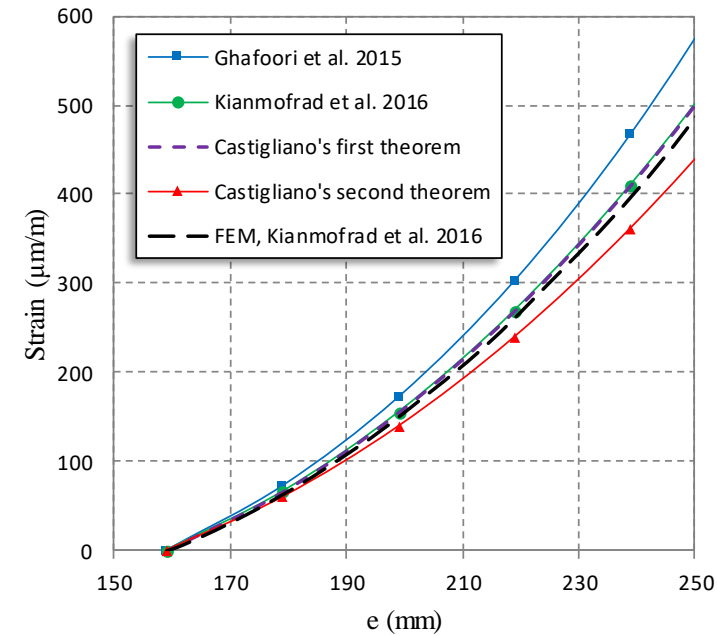
Figure 11 illustrates the strain in different components of the example steel beam reinforced using the TPUR system as a function of deviator height. Figure 11a shows the strain in the beam's upper flange, where it can be seen that the strain obtained using

Castigliano's second theorem is nearly 13% less than that obtained using either Castigliano's first theorem or the flexibility method. When using rigid beam assumption, this strain is predicted around 15.5% higher for $e = 250$ mm (which corresponds to a 60% prestress in the CFRP plate) than when using the more exact methods. For lower values of e , the difference between the various methods becomes less significant. For example, when $e = 180$ mm (which is equivalent to a 10% prestress in the CFRP plate), the difference between the rigid beam assumption and the more exact methods is nearly 10%. The same relationship holds true in figure 11b, which illustrates the calculated tension in the lower flange of the beam. The strain in this component when using the rigid beam assumption is around 10 to 15% larger (depending on the value of e) than the value determined using the more exact methods, while the strain obtained using Castigliano's second theorem is the same range smaller than the value obtained using more exact methods. Additionally, the overall tension and strain in the lower flange (i.e., the compression flange) is higher than in the upper flange (i.e., the tension flange) during

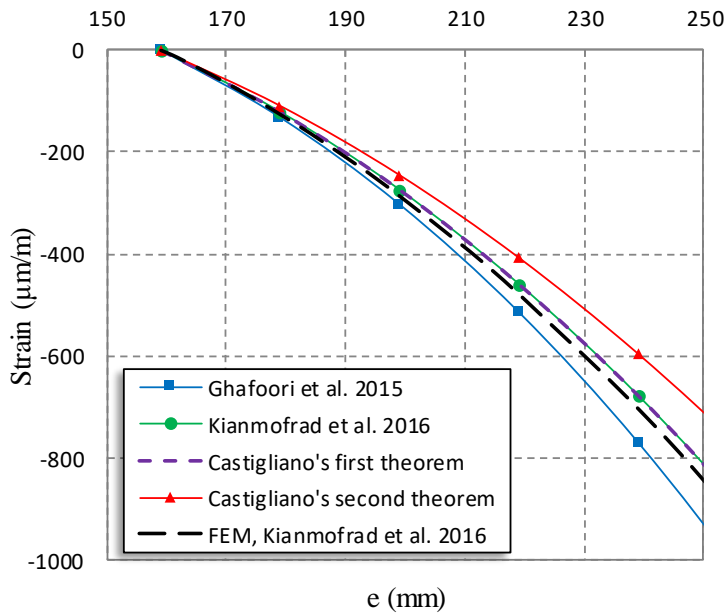
pre-stressing due to tensile force in the CFRP plate, T , transferred into the beam as a compressive axial force.

Figure 11c shows the calculated strain in the CFRP plate, which, when using the rigid beam assumption, is between 10 to 15.4% larger (depending on the value of e) than the value obtained using the more precise methods, while the strain obtained using

Castigliano's second theorem is smaller than the more precise value given by either Castigliano's first theorem or the flexibility method. As can be seen from Figure 11a-c, one noteworthy aspect of this strengthening system is that the tension in the CFRP plate is much higher (by a factor of about 10) than the tension in the beam components.



(a)



(b)

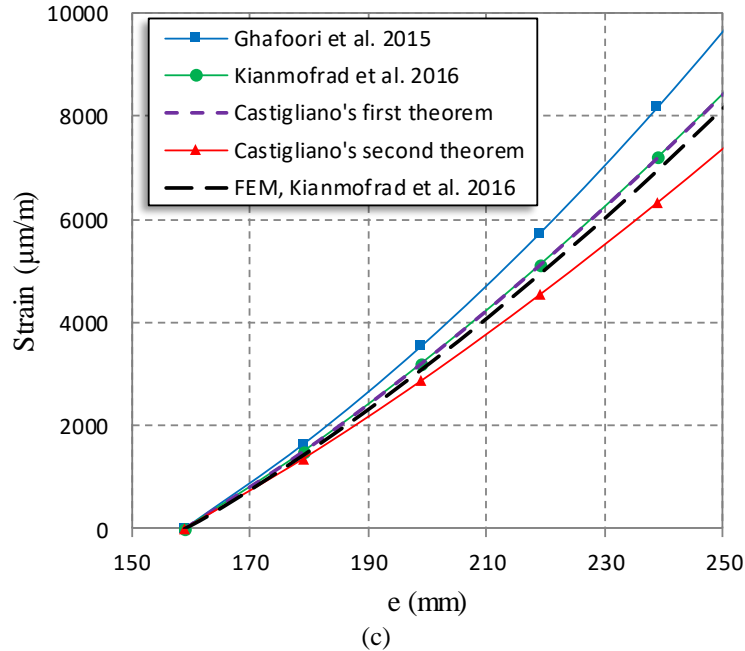


Fig. 11. Strain in: a) the upper, b) the lower flange of the beam and c) the CFRP plate, in terms of the deviator height, e

CONCLUSIONS

In this paper, the applications, as well as the advantages and disadvantages, of different PUR systems for retrofitting were discussed. To provide a basis for the assessment of the relative efficacy of different analytical solutions for describing these PUR systems, several analytical approaches were employed to predict the linear-elastic behavior of a steel I-beam retrofitted using a TPUR system and their results compared. To this end, two energy approaches based on Castigliano's first and second theorems were introduced. The results of these methods were compared to each other, and with results of methods proposed in other research, specifically the flexibility (or force) method and the rigid-beam assumption method.

As expected, the analytical simulations based on Castigliano's first theorem showed good agreement with the flexibility method. Because these methods are applicable to both linear and non-linear systems, they are the most appropriate and accurate solutions for PUR systems, which exhibit a geometrically

non-linear behavior during prestressing. For engineering purposes, however, there is a balance to be struck between accuracy, expense, and time. Accordingly, in use cases such as the initial estimation of retrofitting system performance, using simplified methods (such as Castigliano's second theorem) or simplifying assumptions (such as the rigid-beam assumption) can be beneficial as they produce a solution with an acceptable degree of precision with considerably less effort.

It is determined in this study that Castigliano's second theorem, which is not intended for use in non-linear problems, produces a level of error between 10 to 15%, depending on the CFRP prestress level, and predicts lower tension than present in reality and given by the more exact methods. The same levels of error are present when using the rigid-beam assumption, which predicts lower flexibility and higher tensile force than actually present. While this degree of error does reflect a certain inaccuracy, it is generally acceptable in practical engineering applications.

REFERENCES

- Al-Emrani, M. and Kliger, R. (2006). "Analysis of interfacial shear stresses in beams strengthened with bonded prestressed laminates", *Composites Part B: Engineering*, 37(4), 265-272.
- Aljabar, N.J., Zhao, X.L., Al-Mahaidi, R., Ghafoori, E., Motavalli, M. and Koay, Y.C. (2017). "Fatigue tests on UHM-CFRP strengthened steel plates with central inclined cracks under different damage levels", *Composite Structures*, 160, 995-1001.
- Aljabar, N.J., Zhao, X.L., Al-Mahaidi, R., Ghafoori, E., Motavalli, M. and Powers, N. (2016). "Effect of Crack Orientation on Fatigue Behaviour of CFRP-Strengthened Steel Plates", *Composite Structures*, 152, 295-305.
- Benachour, A., Benyoucef, S. and Tounsi, A. (2008). "Interfacial stress analysis of steel beams reinforced with bonded prestressed FRP plate", *Engineering Structures*, 30(11), 3305-3315.
- Boresi, A.P., Schmidt, R.J. and Sidebottom, O.M. (1993). *Advanced mechanics of materials*, Wiley New York.
- Fernando, D., Schumacher, A., Motavalli, M., Teng, J. G., Yu, T. and Ghafoori, E. (2010). "Fatigue strengthening of cracked steel beams with CFRP plates", *ASME International Mechanical Engineering Congress and Exposition, Proceedings (IMECE)*, 271-276.
- Ghafoori, E. (2013). "Interfacial stresses in beams strengthened with bonded prestressed plates", *Engineering Structures*, 46, 508-510.
- Ghafoori, E. (2015). "Fatigue strengthening of metallic members using un-bonded and bonded CFRP laminates." *PhD Thesis, ETH-Zurich*, (<http://dx.doi.org/10.3929/ethz-a-010453130>).
- Ghafoori, E. and Motavalli, M. (2011). "Analytical calculation of stress intensity factor of cracked steel I-beams with experimental analysis and 3D digital image correlation measurements", *Engineering Fracture Mechanics*, 78(18), 3226-3242.
- Ghafoori, E. and Motavalli, M. (2013). "Flexural and interfacial behavior of metallic beams strengthened by prestressed bonded plates", *Composite Structures*, 101, 22-34.
- Ghafoori, E. and Motavalli, M. (2015a). "Innovative CFRP-prestressing system for strengthening metallic structures", *Journal of Composites for Construction*, 19(6), 04015006.
- Ghafoori, E. and Motavalli, M. (2015b). "Lateral-torsional buckling of steel I-beams retrofitted by bonded and un-bonded CFRP laminates with different pre-stress levels: Experimental and numerical study", *Construction and Building Materials*, 76, 194-206.
- Ghafoori, E. and Motavalli, M. (2015c). "Normal, high and ultra-high modulus CFRP laminates for bonded and un-bonded strengthening of steel beams", *Materials and Design*, 67, 232-243.
- Ghafoori, E. and Motavalli, M. (2016). "A retrofit theory to prevent fatigue crack initiation in aging riveted bridges using carbon fiber-reinforced polymer materials", *Polymers*, 8, 308.
- Ghafoori, E., Motavalli, M., Botsis, J., Herwig, A. and Galli, M. (2012). "Fatigue strengthening of damaged metallic beams using prestressed unbonded and bonded CFRP plates", *International Journal of Fatigue*, 44, 303-315.
- Ghafoori, E., Motavalli, M., Nussbaumer, A., Herwig, A., Prinz, G. and Fontana, M. (2015a). "Determination of minimum CFRP pre-stress levels for fatigue crack prevention in retrofitted metallic beams", *Engineering Structures*, 84, 29-41.
- Ghafoori, E., Motavalli, M., Nussbaumer, A., Herwig, A., Prinz, G.S. and Fontana, M. (2015b). "Design criterion for fatigue strengthening of riveted beams in a 120-year-old railway metallic bridge using prestressed CFRP plates", *Composites Part B: Engineering*, 68, 1-13.
- Ghafoori, E., Motavalli, M., Zhao, X. L., Nussbaumer, A. and Fontana, M. (2015c). "Fatigue design criteria for strengthening metallic beams with bonded CFRP plates." *Engineering Structures*, 101, 542-557.
- Ghafoori, E. and Motavalli, M. (2015d). "Innovative CFRP-prestressing system for strengthening metallic structures", *Journal of Composites for Construction*, 19(6), 04015006.
- Ghafoori, E., Prinz, G.S., Mayor, E., Nussbaumer, A., Motavalli, M., Herwig, A. and Fontana, M. (2014). "Finititione element analysis for fatigue damage reduction in metallic riveted bridges using prestressed CFRP plates", *Polymers*, 6(4), 1096-1118.
- Ghafoori, E., Schumacher, A. and Motavalli, M. (2012). "Fatigue behavior of notched steel beams reinforced with bonded CFRP plates: Determination of prestressing level for crack arrest", *Engineering Structures*, 45, 270-283.
- Hibbeler, R.C. (2014). *Structural analysis*, Pearson Education, Inc., Upper Saddle River, New Jersey 07458.
- Hosseini, A., Ghafoori, E., Motavalli, M. and Nussbaumer, A. (2016). "Stress analysis of unbonded and bonded prestressed CFRP-strengthened steel plates", *8th International Conference on Fiber Reinforced Polymer (FRP) Composites in Civil Engineering (CICE2016)*, 14-16 December 2016, Hong Kong, China.
- Huawen, Y., König, C., Ummenhofer, T., Shizhong, Q. and Plum, R. (2010). "Fatigue performance of

- tension steel plates strengthened with prestressed CFRP laminates", *Journal of Composites for Construction*, 14(5), 609-615.
- Kerboua, B. and Benmoussat, A. (2011). "Strengthening of damaged structures with bonded prestressed FRP composites plates: An improved theoretical solution", *Journal of Composite Materials*, 45(5), 499-512.
- Kianmofrad, F., Ghafoori, E., Elyasi, M.M., Motavalli, M. and Rahimian, M. (2017). "Strengthening of metallic beams with different types of pre-stressed un-bonded retrofit systems", *Composite Structures*, 159, 81-95.
- Park, S., Kim, T., Kim, K. and Hong, S.-N. (2010). "Flexural behavior of steel I-beam prestressed with externally unbonded tendons", *Journal of Constructional Steel Research*, 66(1), 125-132.
- Ponnada, M.R. and Vipparthy, R. (2013). "Improved Method of Estimating Deflection in Prestressed Steel I-Beams", *Asian Journal of Civil Engineering (BHRC)*, 14(5), 765-772.
- Rahimian, M. and Ghorbani Tanha, A.K. (2002). *Strutural analysis*, Sanjesh, Tehran, Iran, (in Persian).
- Rashid Dadash, P. and Ramezaniapour, A.A. (2014). "Hybrid fiber reinforced concrete containing pumice and metakaolin", *Civil Engineering Infrastructures Journal*, 47(2), 229-238.
- Saleh Jalali, R. and Shadafza, E. (2016). "The elastic modulus of steel fiber reinforced concrete (SFRC) with random distribution of aggregate and fiber", *Civil Engineering Infrastructures Journal*, 49(1), 21-32.
- Schnerch, D. and Rizkalla, S. (2008). "Flexural strengthening of steel bridges with high modulus CFRP strips", *Journal of Bridge Engineering*, 13(2), 192-201.
- Soranakom, C. and Mobasher, B. (2007). "Closed-form solutions for flexural response of fiber-reinforced concrete beams", *Journal of Engineering Mechanics*, 133(8), 933-941.
- Täljsten, B., Hansen, C.S. and Schmidt, J.W. (2009). "Strengthening of old metallic structures in fatigue with prestressed and non-prestressed CFRP laminates", *Construction and Building Materials*, 23(4), 1665-1677.
- Tavakkolizadeh, M. and Saadatmanesh, H. (2003). "Fatigue strength of steel girders strengthened with carbon fiber reinforced polymer patch", *Journal of Structural Engineering*, 129(2), 186-196.
- Timoshenko, S.P. and Young, D.H. (1965). *Theory of structures*, McGraw-Hill, New York.
- U.S. Department of Transportation. (1986). "Highway bridge replacement and rehabilitation program", Federal Highway Administration, Bridge Division Office of Engineering.